Available online at www.sciencedirect.com
ScienceDirect
Nuclear Energy and Technology 1 (2015) 14–19

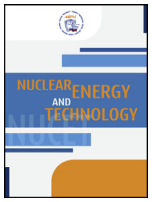

www.elsevier.com/locate/nucet

Comparative analysis of MCNPX and GEANT4 codes for fast-neutron radiation treatment planning

A.N. Solovyev*, V.V. Fedorov, V.I. Kharlov, U.A. Stepanova

Federal State Institution (Medical Radiological Research Center) of the Ministry of Healthcare of the Russian Federation, 4, Korolev st., Obninsk 249036, Kaluga reg., Russia

Available online 28 February 2016

Abstract

The paper presents a comparative analysis of the MCNPX and GEANT4 simulation tools for the beam therapy fast neutron transport calculation problems. Groups of model experiments are described which compare the absorbed energy calculated values obtained on different types of phantoms and the rate of calculation for both simulation tools is assessed depending on the variation in the phantom and source parameters. The results of the studies can be used as the basis for the fast-neutron treatment radiation planning.

Keywords: Radiation therapy; Radiation treatment planning; Monte Carlo method.

Introduction

Quantitative assessment of the energy absorbed in a substance is employed on a great scale, as the absorbed dose in different organs and body parts of a patient during actual irradiation can be determined from the quantity of this energy. This is the key task at the patient pre-irradiation preparation stage [1].

At present, there are only a number of centers in the world offering fast-neutron beam therapy services. These include three laboratories in the USA, two in Japan, one in Germany and two in Russia [2,3]. In Russia, joint activities with VNIIA are under way at the Obninsk Medical Radiological Scientific Center of the Russian Ministry for Public Health to create a therapeutic facility for therapy by neutrons with the energy of 14 MeV [5]. The key component of this facility is a neutron generator. It operates based on the $^{3}T(d,n)^{4}He$ reaction and generates a monoenergy flux of radiation. This makes the generator superior to the reactor therapeutic facilities, such as FRMII in Germany [6], where, apart from 14MeV neutrons, low-energy neutrons are present, starting from thermal neutrons. Such spectrum limits to a certain extent the range of actual medical applications for the facilities of this type and a great deal of engineering and technical effort is required to make it fit for use.

This study has assessed the action of 14 MeV neutrons on different types of phantoms. Two groups of model experiments were conducted for each of the simulation tools. In experiments of group 1, the results of a calculation on a water voxel phantom of different configurations were compared, including depth and longitudinal isodose distributions and surface effects of the secondary protons formed as the result of the neutron-substance interaction. In group 2, the variation in the calculation rate, depending on the phantom composition, and the change in the source configuration, were compared. As options, a water phantom, a tissue-equivalent phantom and a number of real human phantoms, obtained based on different DICOM-images, were compared. Different parameters of the source are coupled with regard for the impact from the neutron generator as such, and from the medical therapeutic facility comprising the generator and the collimator [7,8].

The requirement for such comparison has emerged from a discrepancy [9] in the experimental data and the calculation model built in the MCNP5 environment. The results of the experiment have led to the need for reassessing the capabilities of the MCNP5 code, which, having a limited range of particles,

* Corresponding author.
E-mail addresses: salonf@googlemail.com (A.N. Solovyev), mrvvf@yandex.ru (V.V. Fedorov), vkharlov@mrrc.obninsk.ru (V.I. Kharlov), oktan9@yandex.ru (U.A. Stepanova).

Peer-review under responsibility of National Research Nuclear University MEPhI (Moscow Engineering Physics Institute).
http://dx.doi.org/10.1016/j.nucet.2015.11.004

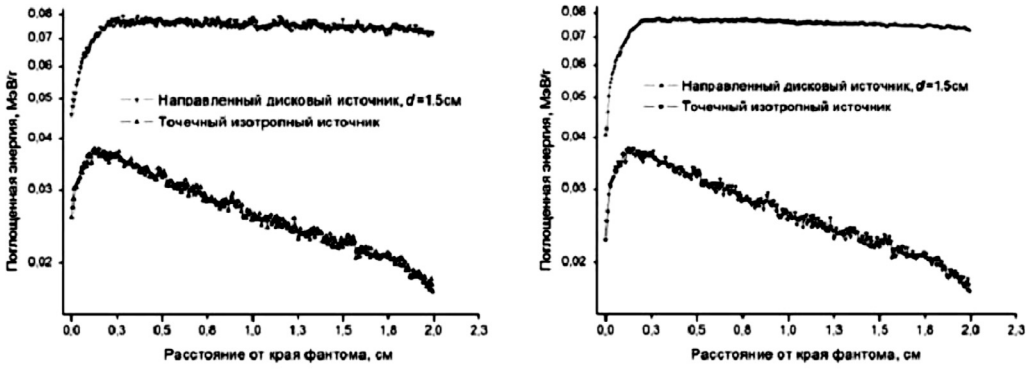

Поглощенная энергия, МэВ/г = Absorbed energy, MeV/g
Направленный дисковый источник, d = 1.5 см = Directed disk source, d = 1.5 cm
Точечный изотропный источник = Point isotropic source
Расстояние от края фантома, см = Distance from phantom edge, cm

Fig. 1. Depth distribution of absorbed energy in the water phantom calculated using MCNPX (left) and GEANT4 (right). The distance from the source is 5 cm. The neutron energy is 14 MeV. The neutron energy flux density is 10^{11} n/s.

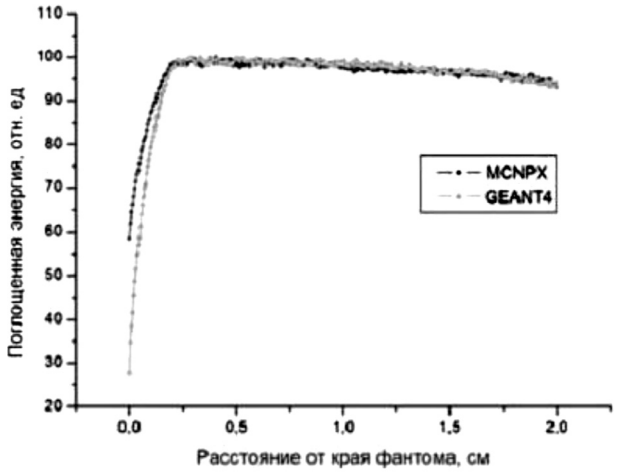

Поглощенная энергия, отн. ед. = Absorbed energy, rel. units
Расстояние от края фантома, см = Distance from phantom edge, cm

Fig. 2. A comparative analysis of the total absorbed energy depth distribution (in relative units) in the water phantom. Directed disk source, d = 1.5 cm. The neutron energy is 14 MeV.

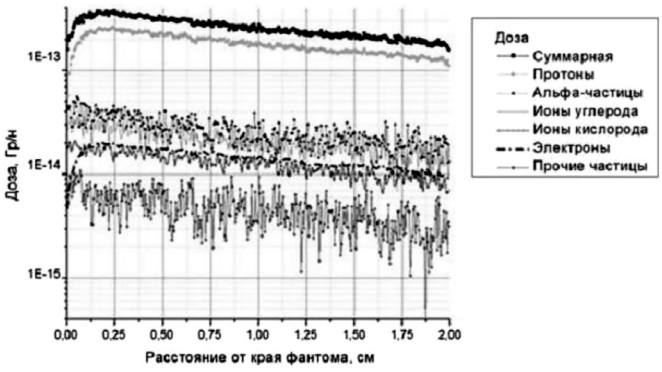

Доза, Гр/н = Dose, Gy/n
Расстояние от края фантома, см = Distance from phantom edge, cm
Доза = Dose
Суммарная = Total
Протоны = Protons
Альфа-частицы = Alpha particles
Ионы углерода = Carbon ions
Ионы кислорода = Oxygen ions
Электроны = Electrons
Другие частицы = Other particles

Fig. 3. Spectral distribution of absorbed energy from secondary particles.

treats the energy released in a particular cell of the phantom as neutron energy without secondary particles, specifically protons, taken into account. This explains the selection of the MCNPX code which enables energy from secondary protons (being the major contributors) to be counted, and of the GEANT4 code which counts absolutely all types of interactions and does not use kerma approximation.

Tools and methods

The MCNPX v.2.4.5e [10] and GEANT4.9.5-1 [11] software products were used in the problem under consideration.

Monte-Carlo N-Particle Transport Code (MCNP) is a family of codes for simulating the transport of ionizing radiation (neutrons, photons, electrons and others) in material systems using Monte-Carlo methods. MCNPX was developed at Los Alamos National Laboratory in the USA in the ANSI C and FORTRAN programming languages. The code simulates the interaction of particles (neutrons, photons and electrons) with the substance of the system. The scattering and capture reactions, as well as the reaction of nuclei fission by neutrons are considered. It also generates a source of secondary particles formed in nuclear reactions (fission neutrons, photons, electrons). The code is used for problem solving in the fields of nuclear reactor physics, radiation protection and medical radiology [2].

This study used parameters of particles (specified by the phys:x directives) [10] other than default values. In particular, special parameters were set for neutron, photon, electron and proton physics: analog simulation was enabled for all types of particles (that is, use of purely statistical methods for dispersion reduction was disabled), the neutron decay capability was disabled, photonuclear reactions on photons were disabled, and

continuous deceleration approximation was used for the electron and proton calculation.

GEANT4 (GEometry ANd Tracking) is a code for simulating the passage of elementary particles through a substance using Monte-Carlo methods. It was developed at CERN in C++, an object-oriented programming language. GEANT4 makes it possible to simulate particles in a very broad energy range (from several electronvolts to many gigaelectronvolts). Unlike MCNP, it allows taking into account during simulation all secondary particles generated in nuclear reactions of primary particles with the substance, and offers a broad variety of capabilities for the acquisition of all kinds of information (the energy generated in the preset amount, the absorbed dose, the particle flux, the track lengths and so on) [11]. The study used the GEANT 4.9.5 code version and an in-house set of physical interactions, G4VModularPhysicsList, composed based on the recommendations set forth in the user guide [11].

Calculations were performed without using parallel calculation techniques because this could not be done in MCNPX without recompiling the initial codes not supplied to Russia and the CIS countries for political reasons. All calculations were performed on one machine with eight Intel Xeon processors (a time step frequency of 2.8 GHz), which made it possible to start simultaneously several calculations, one per each physical processor, without a loss in efficiency. The Origin software product was used for diagram plotting. An in-house code written in the Python language [12] was used to plot isodose distributions using the Numpy [13] and Matplotlib [14] libraries.

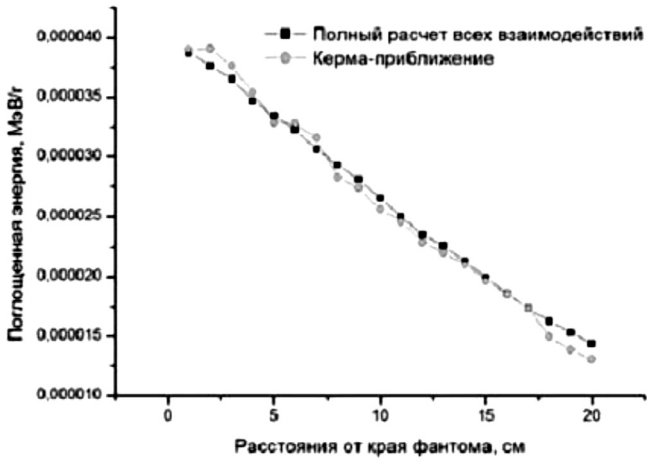

Поглощенная энергия, МэВ/г = Absorbed energy, MeV/g
Полный расчет всех взаимодействий = Full calculation of all interactions
Керма-приближение = Kerma approximation
Расстояние от края фантома, см = Distance from phantom edge, cm

Fig. 4. A comparison of the two types of MCNPX calculations on a human phantom of 20 × 20 × 20 cm^3: cell size – 0.5 cm; calculation time – 4157 min (full calculation of all interactions – 360 million histories, average error – 8%; calculation in kerma approximation – 870 million histories, average error – 5%).

Group 1 of model experiments: water phantom

Water phantom is a traditional base model of the human body for radiation treatment planning. Water phantoms exactly had been used before computer simulation tools came into being: the isodose distribution pattern, based on experimental data, was drawn by tracing on one tomographic image of the area around the patient's tumor [1]. It should be noted that such techniques are used in the era of computer-aided simulation as well – there are groups of methods based on the adjustment of the absorbed energy (and, consequently, the absorbed dose) depending on the ratio of the tissue density to the density of water. No interaction of neutrons with the human body tissues can be calculated accurately using these methods. Water phantom simulation also exhibits the results observed in real experiments: the maximum absorbed energy from neutrons with the energy of 14 MeV (and, as a consequence, the maximum dose) is formed not at the phantom edge nearest to the source, but at a depth of about two millimeters. Figs. 1 and 2 present diagrams of the energy absorbed in a substance versus the depth inside the phantom.

Looking at the contribution made by different particles to the total absorbed dose, one will obtain the depth distribution pattern shown in Fig. 3.

However, such detailed calculation (a grid pitch of 5 μm was used in some of the calculations) will not have a practical application in actual clinical environments due to high resource intensity and limited resolution of tomographic images (the image

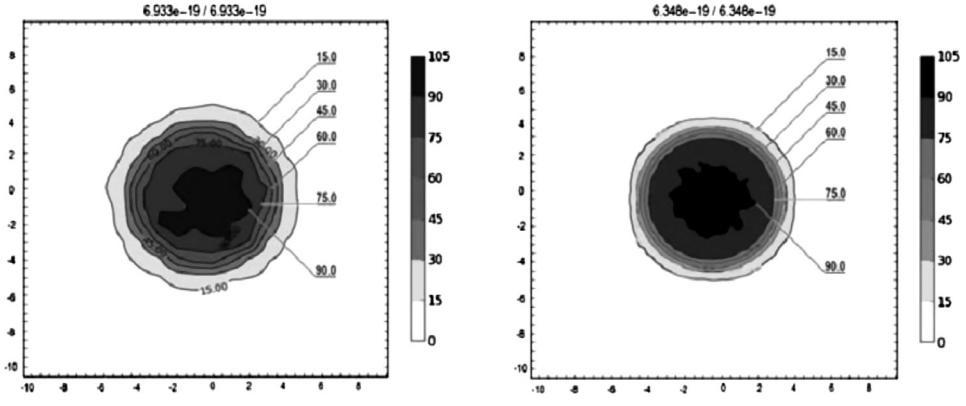

Fig. 5. A transverse isodose distribution based on results of simulations in the GEANT4 (left) and MCNPX (right) environments, the layer nearest to the source (axes – distances, cm; isolines – 100%-normalized absorbed energy; top –maximum absorbed dose in the layer/maximum absorbed dose on the phantom, Gy/n).

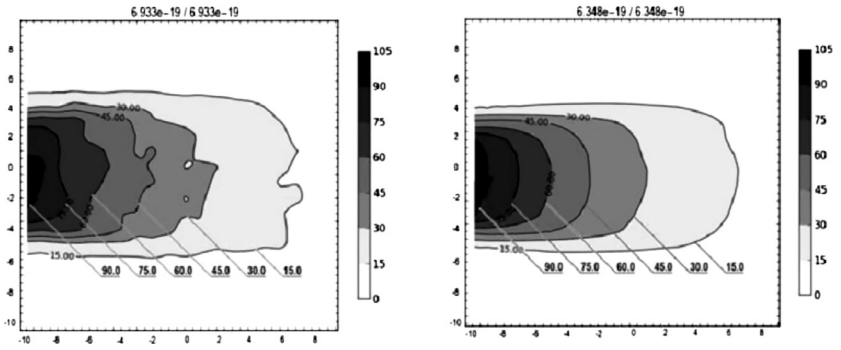

Fig. 6. A longitudinal isodose distribution based on results of simulations in the GEANT4 (left) and MCNPX (right) environments, central layer (axes – distances, cm; isolines – 100%-normalized absorbed energy; top – maximum absorbed dose in the layer/maximum absorbed dose on the phantom, Gy/h).

resolution is normally 0.7 mm/pixel). This is exactly the reason for the problem of water phantom investigations remaining on the agenda: a water phantom can be used to obtain the general nature of the depth curve behavior (and, as a consequence, of the isodose distribution), to count the percentage of the dose "fall-off" on the surface, and to use, after this, techniques to identify the surface and boundary layers on a real human phantom and to recount the doses calculated by faster methods depending on the percentage obtained. In particular, the calculation of the energy absorbed by a substance in kerma approximation gives perfect characteristics deeply inside the phantom, while exhibiting excellent performance (Fig. 4).

Longitudinal and transverse isodose distributions calculated for a water phantom of $10 \times 10 \times 10$ cm^3 (the phantom cell size is 0.5 cm) are presented in Figs. 5 and 6. The source is of a unidirectional disk type, $d_{sou} = 0.75$ cm. The distance from the source is 17 cm.

Therefore, one can note that MCNPX and GEANT4 display good results in a water phantom simulation which fit each other and can be used for further investigations.

Group 2 of model experiments: other phantoms and simulation on the theraeutic facility

Model experiments in group 2 were conducted to identify the features of the media calculations, including tissue-equivalent and real ones, obtained based on tomographic images.

The first experiment consisted in a simple substitution of the phantom material from water to a generalized soft tissue of the ICRU standard with a density of 1.06 g/cm^3 (its components are presented in Table 1).

Despite the fact that tissue contains more hydrogen than water, the contribution of secondary protons did not vary. Fig. 7 presents a comparative diagram showing the percentage of the proton contribution to the total absorbed energy. The observed data scatter in tissue is explained by poor statistics. The action of neutrons with the energy 14 MeV was comparatively overviewed by the authors to the full extent in [15].

The configuration closest to the life-size one was calculated within this group of model experiments: tomographic images

Table 1
Material composition of the generalized soft tissue.

Element	Mass fraction of element (%)
H (hydrogen)	10.20
C (carbon)	14.3
N (nitrogen)	3.4
O (oxygen)	70.8
Na (sodium)	0.2
P (phosphorus)	0.3
S (sulfur)	0.3
Cl (chlorine)	0.2
K (potassium)	0.3

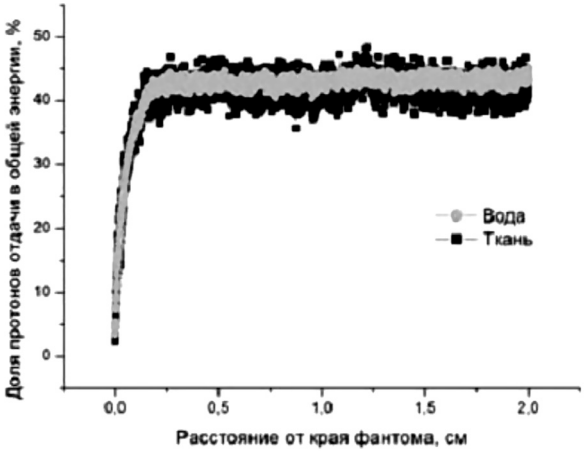

Доля протонов отдачи в общей энергии, % = Contribution of recoil protons to total energy, %
Вода = Water
Ткань = Tissue
Расстояние от края фантома, см = Distance from phantom edge, cm

Fig. 7. A comparative contribution of recoil protons to the total absorbed energy in water and in soft tissue (MCNPX calculation; phantom layer size – 5 μm).

of the patient, in the form processed and reduced to standard tissues, were used as the phantom. The tomographic images were reduced to the calculation model using two methods. Method 1 was similar to that used in the SERA planning system [16]. Method 2 is used in one of the examples supplied together with the GEANT4 code and consists in the following: the voxel value is obtained based on an expanded table of materials after

Table 2
Summary table of the experimental results.

Experiment, phantom parameters		Number of histories (min)	Calculation time (min)	Average error (%)	Note
Water phantom					
MCNPX	Monolayers, 400 × 50 μm^2	6	82/106	1/0.8	Point/disk source
	20 × 20×20[a] 0.5 × 0.5 × 0.5 cm^3	500	2400/3638	4/6	Generator with no collimator/with collimator
	64 × 64×35[a] .25 × .25 × .6 cm^3	200	2800	5	Water equivalent phantom
GEANT4	Monolayers, 400 × 50 μm^2	6	140/154	2	Point/disk source
	20 × 20×20[a] .5 × .5 × .5 cm^3	500	2500/4100	—[b]	Generator with no collimator/with collimator
	64 × 64×35[a] .25 × .25 × .6 cm^3	200	3100	—[b]	Water equivalent phantom
Tissue-equivalent phantom					
MCNPX	Monolayers, 4000 × 5 μm^2	1200	8648	2	Disk source for comparison with water
	20 × 20×20[a] 0.5 × 0.5 × 0.5 cm^3	18	1400	6	Isodose calculation
GEANT4	Monolayers, 4000 × 5 μm^2	1200	9500	2	Disk source for comparison with water
	20 × 20×20[a] .5 × .5 × .5 cm^3	18	1480	7	Isodose calculation
Real phantom					
MCNPX	64 × 64×35[a] .25 × .25 × .6 cm^3	560/400/1800	6140	4/5/1	Human head phantom, 1/2/ker-approximation methods
GEANT4	64 × 64×35[a] 0.25 × 25×6 cm^3	400	7000/7180	—[b]	Human head phantom, 1/2 methods

[a] – dimensions in voxels.
[b] – these examples were not modified for the statistical error count.

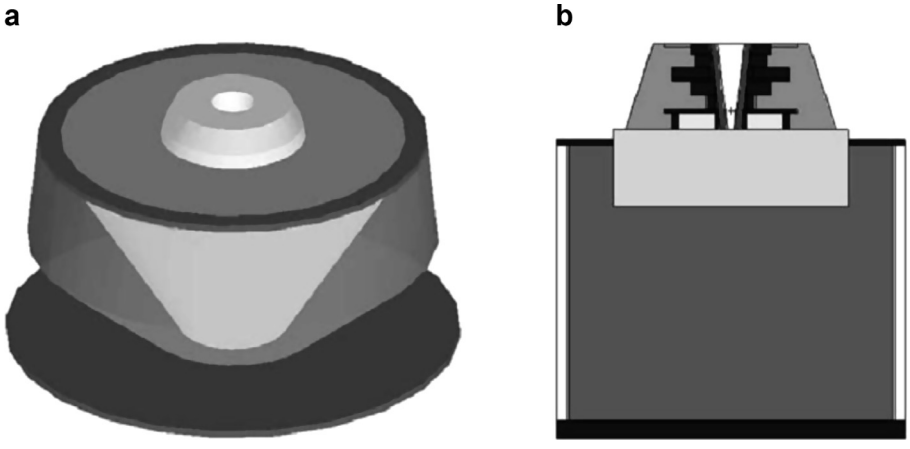

Fig. 8. A cross-section of the NG-24 generator and of the in-house collimator as visualized in the GEANT4 (a) and Vised (b) environments.

the average density of the tissue in the image is found [11]. This technique is limited greatly; specifically, it will not be correct to use a similar set of tissues for the head and abdominal cavity images. However, the total quantity of materials in the final calculation turns out to be smaller than in method 1. An own implementation of the two methods was written in the Python language [12] using the Numpy [13] and PIL [17] libraries. However, as shown by the calculation results, method 2, despite a smaller quantity of final materials, turns out to be 20% as slow on the average as method 1, and this is the case with both the

MCNPX code and the GEANT4 code. Besides, voxel phantoms can be used to calculate the associated radiological problems, to assess the risk and the protection level, and so on [18].

The closing experiment in this group was conducted for taking into account the source configuration effects. A calculation model of the NG-24 generator, both with and without a dedicated collimator, was used. Standard tools of both simulation packages were used to transport and rotate the "generator-collimator" assembly to follow the calculation rate variation relative to the base position (the assembly was perpendicular to the phantom). The experiment results have shown that MCNPX (greatly) and GEANT4 (to a smaller extent) were sensitive to the rotation angle. Since the rotation angles are known in advance and are preset at the pre-calculation planning stage, further studies will have the purpose of creating an algorithm for transforming the initial 3D DICOM-volume so that the resultant equivalent phantom was always perpendicular to the source of radiation. Fig. 8 shows the collimator cross-section in the GEANT4 built-in environment (no materials are highlighted) and in Vised, a program supplied together with the MCNP code.

Consolidated data for all groups of experiments are presented in Table 2.

Conclusions

After analyzing the resultant data, the following can be stated.

1. A calculation in kerma approximation works four times as fast on the average (the number of histories is four times as large with the same calculation time) and the accuracy of generated results is three times as high (the average error of 0.3 against 1.0 in the full calculation on the water phantom). The advantage of such calculation is that it can be performed using the MCNP5 code, which may be in turn devoid of parallelism through MPI (Message Passing Interface), one of the classic approaches to the development of cluster high-capacity calculations. This calculation is limited by that it cannot take into account the effects on the interface of highly dense media (water-tissue, tissue-bone); it will be exactly in these regions that the maximum amount of the absorbed energy will leave the surface to go into the depth.
2. The substitution of water for any multicomponent structure (e.g. tissue) causes the calculation in both environments to slow down by 40 to 50% on the average, while the error does not practically vary.
3. The calculation of the voxel phantom, built based on tomographic images using method 1 (with a large number of materials), is faster in both environments than when method 2 is used, but, on the whole, the slowdown relative to the tissue-equivalent phantom is insignificant.

It can be concluded that, despite all advantages of fast neutrons with the energy of 14 MeV [4,5,9], the application of these calls for tougher requirements to the computational radiation treatment planning and simulation tools, exactly what has been demonstrated by this study. One needs to look for new tradeoffs between the calculation accuracy, the correct assessment of the dose on the body surface and the simulation time which can be also a critical factor in the commissioning of such therapeutic facilities. This gives rise to a whole range of problems resolved in further investigations. From this point of view, the GEANT4 environment seems to be more promising, since users are in a position to modify the initial code to make it fit their own needs, as well as in connection with the fact that there is a large number of publications describing this environment, including those pertaining to the use of cloud technologies in calculations. Further investigations will consider questions dealing with the best possible presentation of human phantoms in simulation systems, as well as with distributed calculations as part of a single hadronic beam therapy software and hardware package.

References

[1] G.E. Trufanov, M.A. Asaturyan, G.M. Gharinov, Luchevaya Trapiya – Tom 2 [Radiation therapy – Part 2], GEOTAR-Media Publ., Moscow, 2007, p. 195. (in Russian).
[2] Wikipedia, the free Encyclopedia. Available at: http://ru.wikipedia.org, http://en.wikipedia.org
[3] A.S. Saenko, Yu.S. Mardinskiy, S.E. Ulyanenko, Otchet o NIR. Razvitie Biomedicinskih Osnov Ispolzovaniya Reaktornih Neitronov dlya Distancionnoi, Neutronzahvatnoi i Sochetannoi Luchevoi Terapii [Research results. The Biomedical Basis Development for Reactor Neutrons Usage in External Beam Radiotherapy, Neutron-capture Therapy and Concomitant Therapy.], MRRC, Obninsk, 2004, p. 300. (in Russian).
[4] A.F. Tsyb, S.E. Ulyanenko, Yu.S. Mardinskiy, Neitroni v Lechenii Zlokachestvennih Novoobrazovaniy [Neutron in Malignancies Treatment], MRRC, Obninsk, 2004, p. 94. (in Russian).
[5] A.I. Brovin, V.M. Lityaev, A.A. Lichagin, S.N. Koryakin, A.N. Solovyev, S.E. Ulyanenko, in: Proceedings of Conference on Portable Neutron Generators and Technologies on their Basis, Moscow, 2012, pp. 4–5.
[6] Garny Sylvia, Rьhm Werner, et al., Radiat. Oncol. 6 (2011) 163.
[7] V.M. Lityaev, A.N. Solovyev, in: Proceedings of the Conference on Portable Neutron Generators and Technologies on their Basis, Moscow, 2012, p. 27.
[8] Lityaev V.M., Ulyanenko S.E., Gorbushin N.G. Ustroistvo Dlya Luchevoi Terapii Bistrimi Neitronami [The Fast Neutron Radiation Treatment Facility]. Parent RF, no. 2442620, 2012.
[9] V.M. Lityev, A.A. Lychagin, V.I. Potetnya, A.N. Solovyev, S.E. Ulyanenko, V.I. Harlov, in: Proceedings of the Conference on Portable Neutron Generators and Technologies on their Basis, Moscow, 2012, p. 26.
[10] MCNPX Home page. Available at: http://mcnpx.lanl.gov/
[11] Geant4: A Toolkit for the Simulation of the Passage of Particles Through Matter. Available at: http://geant4.cern.ch/
[12] Python. Available at: http://www.python.org/
[13] Numpy. Available at: http://www.numpy.org/
[14] Matplotlib: Python Plotting. Available at: http://matplotlib.sourceforge.net/
[15] U.A. Stepanov, A.N. Solovyev, P.S. Prusachenko, Experimental and Theoretical Biophysics, 13, Puschino, Fix-print Publ., 2013, pp. 127–128. Books of theses(in Russian).
[16] A.N. Solovyev, Inf. Telekommun. Tehnol. (17) (2013) 48–60 (in Russian).
[17] Python Imaging Library. Available at: http://www.pythonware.com/products/pil/
[18] D.N. Moiseenko, U. Kurachenko, Izv. vuzov. Yad. Energ. (4) (2012) 152–160.